CNTF Prevents Development of Outer Retinal Neovascularization Through Upregulation of CxCl10

Felicitas Bucher,[1,2] Edith Aguilar,[1] Kyle V. Marra,[1,3] Julian Rapp,[2] Jakob Arnold,[2] Sophia Diaz-Aguilar,[1,2] Clemens Lange,[2] Hansjürgen Agostini,[2] Günther Schlunck,[2] Andreas Stahl,[4] and Martin Friedlander[1,5]

[1]Department of Molecular Medicine, The Scripps Research Institute, La Jolla, California, United States
[2]Eye Center, Medical Center, Faculty of Medicine, University of Freiburg, Freiburg, Germany
[3]Department of Bioengineering, University of California, San Diego, San Diego, California, United States
[4]Department of Ophthalmology, University Medical Center Greifswald, Greifswald, Germany
[5]The Lowy Medical Research Institute, La Jolla, California, United States

Correspondence: Martin Friedlander, The Scripps Research Institute, 10550 N Torrey Pines Road, La Jolla, CA 92037, USA; friedlan@scripps.edu.

Received: March 28, 2020
Accepted: June 25, 2020
Published: August 11, 2020

Citation: Bucher F, Aguilar E, Marra KV, et al. CNTF prevents development of outer retinal neovascularization through upregulation of CxCl10. *Invest Ophthalmol Vis Sci.* 2020;61(10):20. https://doi.org/10.1167/iovs.61.10.20

Purpose. Ciliary neurotrophic factor (CNTF) is a well-characterized neurotrophic factor currently in clinical trials for the treatment of macular telangiectasia type II. Our previous work showed that CNTF-induced STAT3 signaling is a potent inhibitor of pathologic preretinal neovascular tuft formation in the mouse model of oxygen-induced retinopathy. In this study, we investigated the effect of CNTF on outer retinal and choroidal angiogenesis and the mechanisms that underpin the observed decrease in outer retinal neovascularization following CNTF treatment.

Methods. In the *Vldlr*$^{-/-}$ and laser-CNV mouse models, mice received a one-time injection (on postnatal day [P] 12 in the *Vldlr*$^{-/-}$ model and 1 day after laser in the Choroidal Neovascularization (CNV) model) of recombinant CNTF or CxCl10, and the extent of neovascular lesions was assessed 6 days posttreatment. STAT3 downstream targets affected by CNTF treatment were identified using quantitative PCR analysis. A proteome array was used to compare media conditioned by CNTF-treated and control-treated primary Müller cells to screen for CNTF-induced changes in secreted angiogenic factors.

Results. Intravitreal treatment with recombinant CNTF led to significant reduction in neovascularization in the *Vldlr*$^{-/-}$ and laser-CNV mouse models. Treatment effect in the *Vldlr*$^{-/-}$ was long-lasting but time sensitive, requiring intravitreal treatment before P19. Mechanistic workup in vitro as well as in vivo confirmed significant activation of the STAT3-signaling pathway in Müller cells in response to CNTF treatment and upregulation of CxCl10. Intravitreal injections of recombinant CxCl10 significantly reduced outer retinal neovascularization in vivo in both the *Vldlr*$^{-/-}$ and laser-CNV mouse models.

Conclusions. CNTF treatment indirectly affects outer retinal and choroidal neovascularization by inducing CxCl10 secretion from retinal Müller cells.

Keywords: CNTF, STAT3, angiogenesis, *Vldlr*$^{-/-}$, Müller cells

Age-related macular degeneration (AMD) and diabetic retinopathy (DR) represent common causes of vision loss in the Western world.[1] Anti-VEGF therapy has revolutionized therapeutic options and visual outcomes of patients with vasoproliferative retinopathy.[2] However, some patients with AMD and DR do not benefit from anti-VEGF therapy, and less common vasoproliferative retinopathies such as macular telangiectasia type I or II (MacTel) are not responsive to anti-VEGF therapy, suggesting that underlying mechanisms of neovascularization in these diseases are not completely understood.[3–5] Further research is necessary to either uncover disease-specific mechanisms, as was recently published for MacTel type II,[6] or to identify other common disease- and VEGF-independent angiomodulatory signaling pathways.

The contributions of the neurovascular unit and chronic inflammation to disease development have repeatedly been stressed.[7–9] Neuroprotective as well as inflammation-modulating therapeutic approaches have shown some success in animal models of proliferative retinopathies and small clinical case series but have not yet been successfully translated into clinical routine.[10,11] Ciliary neurotrophic factor (CNTF) is one of the best-studied neurotrophic agents.[12] As a member of the interleukin 6 cytokine family, CNTF is a strong activator of the JAK/STAT3 signaling pathway that plays a crucial role in the mediation of

inflammatory responses. CNTF binds to CNTF–receptor α (CNTF-Rα), which in turn recruits leukemia inhibiting factor receptor β (LifRβ) and glycoprotein 130 (gp130) as receptor subunits with intracellular signaling domains.[13–15] Formation of this heterotrimeric receptor complex then leads to activation of the JAK/STAT3 signaling pathway and STAT3-dependent gene expression. While LifRβ and gp130 are receptor components expressed on a wide variety of cell types, CNTF-Rα is selectively expressed on distinct cell types, including neuroglial cells in the central nervous system.[16,17]

Multiple preclinical studies provided strong support for the use of CNTF in the treatment of neurodegenerative diseases such as retinitis pigmentosa (RP) or glaucoma.[18–21] Encapsulated cell therapy (ECT) devices load cells into a biocompatible polymer capsule to allow continuous release of therapeutic agents into the vitreous upon implantation within the eye. Implantation of ECT using cells transfected to overexpress CNTF showed promise in reducing photoreceptor loss in mouse models of Retinitis pigmentosa (RP).[22] However, the clinical trial for use of this therapy in the treatment of RP did not meet its primary endpoint.[23] Clinical trial phase II data for the treatment of MacTel type II provided strong evidence that a CNTF-releasing device slows down disease progression.[23,24] Despite the advanced stage of clinical testing, the mechanism of CNTF action in the retina remains elusive.

Preclinical data in the retina have shown that retinal ganglion as well as photoreceptor cells express CNTF-Rα in the retina. Müller cells are also known to respond to CNTF treatment.[25] Rhee et al.[26] showed that CNTF-associated signaling in both photoreceptor and Müller cells is necessary to observe a neuroprotective effect in RP models. In a previous study, we showed that CNTF possessed a strong angiomodulatory effect reducing preretinal neovascularization (NV) in the mouse model of oxygen-induced retinopathy (OIR).[27] This effect could be partially attributed to a direct angiostatic effect of CNTF on vascular endothelial cells in the presence of soluble CNTF-Rα. In the current study, we aimed to elucidate whether the observed angiomodulatory effects of CNTF in OIR were model specific or whether CNTF exhibits a generalized angiostatic effect. The therapeutic effects of CNTF were analyzed in the murine *Vldlr*$^{-/-}$ model of intraretinal neovascularization as well as the laser-CNV model of choroidal NV. In this study, we demonstrated that CNTF strongly improved the vascular phenotype of various in vivo angiogenesis models and investigated indirect mechanisms that contribute to CNTF's angiomodulatory effects. Using gene expression assays of CNTF-treated retinas in vivo and Müller cells in vitro, we identified important CNTF-induced STAT3 downstream targets with an angiomodulatory effect.

Material and Methods

Animal Models

All animal work adhered to the National Institutes of Health (NIH) Guide for the Care and Use of Laboratory Animals. All animal protocols were approved by the Scripps Research Institute IACUC (08-0045-4).

Vldlr$^{-/-}$mice: B6;129S7-*Vldlr*^{tm1Her}/J were purchased from The Jackson Laboratory, Bar Harbor, Maine, US. Mice received intravitreal injections of recombinant protein at different concentrations and time points as specified in the figure legends. To allow for within-animal control, contralateral eyes were used for treatment and control (PBS/0.1% BSA) groups. Recombinant proteins used rat recombinant CNTF (CNTF, #557-NT-050; R&D Systems, Wiesbaden-Nordenstadt, Germany) and recombinant murine CxCl10 (500 ng, #250-16; Peprotech, Hamburg, Germany). Intravitreal injections were performed using a sharp 33-gauge Hamilton needle. Eyes were harvested and prepared for further analysis at time points specified. Retinas were stained with Isolectin GS-B4 (#I21412; ThermoFisher Scientific, Waltham, MA, USA) according to the protocol specified on page 7, inversely flatmounted, and imaged using a confocal laser-scanning microscope (LSM 700 or 710; Zeiss, Oberkochen, Germany). The number of tufts was determined by manual selection of tufts on immunofluorescent images of the inverted flatmounts using the Cell Counter plugin provided by ImageJ (NIH, Bethesda, MD, USA).

The laser-CNV model was performed as previously described.[28] Adult C57BL/6 mice at the age of 6 to 8 weeks received three laser burns per eye using a green Argon laser after anesthesia and pupil dilation. The presence of an air bubble was interpreted as a sign of successful of laser impact. C57BL/6 mice received intravitreal injection of recombinant protein 1 day after laser treatment. Mice received treatment in both eyes (CNTF, mrCxCl10, or PBS/0.1% BSA). Eyes were harvested for choroidal flatmounts 7 days after laser. CNV lesion size was measured by quantification of the CNV area.

For retinal development, C57BL/6 mice were treated with intravitreal injections of CNTF (500 ng) or PBS/0.1% BSA (control) at postnatal day (P) 7. Eyes were harvested 5 days after treatment and prepared for retinal whole mounts. The number of vessel junctions and total vessel length were determined using the AngioTool Software.[29]

Cell Culture

Mouse primary Müller cell cultures were isolated according to a previously published protocol.[30] In brief, retinas from P11 mouse pups were harvested and dissociated using the Papain Dissociation system (#LK003150; Worthington Biochemical Corporation, Lakewood, NJ, USA). Primary Müller cells were expanded in growth medium containing recombinant human endothelial growth factor (100 ng/mL, #PHG0311; Thermo Fisher Scientific), Neurobasal-A medium (#10888022; Thermo Fisher Scientific), N2 Supplement (#17502048; Thermo Fisher Scientific), 10% FBS Superior (#S0615; Merck, Biochrome, Berlin, Germany), L-Glutamine (2 mM, #25030081; Thermo Fisher Scientific), and Pen/Strep (#15140122; Thermo Fisher Scientific) and then transferred to differentiation media containing Neurobasal-A medium (#10888022; Thermo Fisher Scientific), 1% FBS Superior (#S0615; Merck, Biochrome), N2 Supplement (#17502048; Thermo Fisher Scientific), L-Glutamine (2 mM, #25030081; Thermo Fisher Scientific), Pen/Strep (#15140122; Thermo Fisher Scientific), and B27 Supplement (50×, #17504044; Thermo Fisher Scientific) for 7 days. Müller cells at passage P2 were used for immunohistochemistry as well as stimulation experiments. To generate Müller cell-conditioned media, passage P2 primary Müller cells were stimulated with 100 ng/mL CNTF or PBS control for 10 minutes. Cells were washed by PBS, and then fresh differentiation media were added and conditioned for 96 hours after stimulation for use in experiment. Human umbilical vein endothelial cells (HUVECs, #2519A; Lonza,

Basel, Switzerland) were cultured in endothelial growth medium 2 (EGM, #CC-3162; Lonza) and used up to passage P6.

Endothelial Proliferation and Spheroid Sprouting Assays

Cell proliferation was measured using an 3-(4,5-Dimethylthiazol-2-yl)-2,5-diphenyltetrazoliumbromid (MTT) assay according to previously published protocols.[31] In brief, following overnight incubation of HUVECs seeded into a 96-well plate, cells were starved for 24 hours in endothelial basal medium with 4% FBS (EBM, #CC-3121; Lonza, Basel, Switzerland) before stimulation for 72 hours with the following recombinant proteins: recombinant human vascular endothelial growth factor 165b (20 ng/mL, #3045-VE; R&D Systems, Minneapolis, MN, USA), recombinant human fibroblast growth factor–basic (bFGF, 50 ng/mL, #100-18B; Peprotech, Hamburg, Germany), and recombinant human CxCl10 (rhCxCl10, 625 nM, #200-12; Peprotech).

The endothelial spheroid sprouting assay was also performed according to well-established techniques.[32,33] Endothelial spheroids were formed in a hanging drop consisting of 500 HUVECs resuspended in EGM with 10% FBS and 0.25% carboxy-methylcellulose (#M0512; Sigma-Aldrich, Darmstadt, Germany). Spheroids were harvested the following day and 30 spheroids were poured into a 0.5-mL collagen I (1.5 mg/mL final concentration, #354236; Corning, Wiesbaden, Germany) in 24-well plates. Spheroid-containing gel solidified at 37°C for 30 minutes and was then stimulated with 100 µL EBM containing recombinant proteins: VEGF (25 ng/mL, #3045-VE; R&D Systems), bFGF (50 ng/mL, #100-18B; Peprotech), and CxCl10 (537.5 ng/mL, #200-12; Peprotech). Images of single spheroids were taken using an inverted light microscope (Zeiss Axio Vert). Total sprout length was determined by using a self-programmed ImageJ macro where sprouts have to be manually labeled using the "straight-line" tool.

Immunohistochemistry

Eyes were harvested and prepared for immunohistochemical analysis as previously described.[34] In brief, for retinal and choroidal flatmount preparations, eyes were fixed in 4% paraformaldehyde for 40 to 60 minutes on ice and incubated overnight with Isolectin GS-IB4 1:200 (# I21412; Thermo Fisher Scientific). For retinal cross sections, whole eyes were harvested 6 hours after intravitreal treatment, fixed in 2% PFA for 1 hour, and then incubated for 24 hours in 20% sucrose. Sections were fixed with 100% ethanol for 10 minutes followed by permeabilization with 0.3% Triton for 30 minutes and then blocked with 10% BSA for 1 hour. Primary Müller cells were fixed for 5 minutes in 100% methanol at –20°C and permeabilized using 0.3% Triton for 20 minutes. Cells were incubated overnight at 4°C with following primary antibodies: pSTAT3 rabbit mAb (#9145; Cell Signaling Technology, Danvers, MA, USA), chicken anti-mouse Gfap Ab (#ab4674; Abcam, Cambridge, UK), rabbit anti-Kir4.1 (KCNJ10) antibody (#APC-035; Alomone Labs, Jerusalem, Israel), rabbit anti-glutaminsynthetase Ab (#ab73593; Abcam), rabbit anti-mouse CRALBP Ab (#MA1-813; Thermo Fisher Scientific). The following secondary antibodies were used: chicken anti-rabbit 568 (#A-21441; Thermo Fisher Scientific) and goat anti-chicken 488 (#A-32931; Thermo Fisher Scientific).

Table. qPCR Primers

Target	Forward Primer 5' → 3'	Reverse Primer 3' → 5'
mbActin	GGC TGT ATT CCC CTC CAT CG	CCA GTT GGT AAC AAT GCC ATGT
mCebpd	CGACTTCAGCGCCTACA TTGA	GAAGAGGTCGGCGAAG AGTT
mCxCl10	CCAAGTGCTGCCGTCA TTTTC	GGCTCGCAGGGATGAT TTCAA
mSocs3	AGCTGGTGGTGAACG CCGTG	GCGTGCTTCGGGGGT CACTC
mVEGF164	GCCAGCACATAGAGAGA ATGAGC	CAAGGCTCACAGTGATT TTCTGG
mCNTF-Rα	TGTCTACACGCAGAAA CACAG	CCCAGACGCTCATACT GCAC
mLIF-R	TACGTCGGCAGACTCG ATATT	TGGGCGTATCTCTCTC TCCTT
mgp130	CCGTGTGGTTACATCTA CCCT	CGTGGTTCTGTTGATGAC AGTG

Western Blot, Protein Array, and ELISA

For all protein assays, single retinas were lysed in T-Per Buffer (#78519; Thermo Fisher Scientific) containing Phosphatase and Proteinase Inhibitor (#78430 and #78427; Thermo Fisher Scientific). Gel electrophoresis was run under denaturing conditions. Proteins were transferred to a nitrocellulose membrane, blocked with 5% skim milk for 1 hour, and incubated overnight at 4°C with the following antibodies: pSTAT3 rabbit mAb (#9145; Cell Signaling Technology), STAT3 (79D7) rabbit mAb (#4904; Cell Signaling), and anti-bActin Ab (#A1978; Sigma, St. Louis, MO, USA).

Müller cell-conditioned media were analyzed using the Mouse Angiogenesis Array Kit Proteome Profiler (#ARY015; R&D Systems). CxCl10 levels were determined using the mouse IP-10 ELISA Kit (CxCl10) (ab214563; Abcam).

Quantitative PCR, mRNA Array

mRNA was isolated according to the manufacturer's instructions using the miRNAeasy Kit (#217004; Qiagen, Hilden, Germany) and transcribed into cDNA using the High Capacity cDNA Reverse Transcription Kit (#4368814; Thermo Fisher Scientific). The following primers were used for quantitative PCR (qPCR) in the Table.

The RT^2 PCR Profiler PCR Array Mouse Il6/STAT3 signaling pathway (#PAMM-160Z; Qiagen) was used for mRNA array analysis.

Statistics

All graphs are presented as scatterplots. For in vivo experiments, graphs represent mean ± SEM. Statistical tests were applied as outlined in the figure legends. For qPCR analyses, graphs are plotted as mean ± 95% CI. Statistical tests were performed on delta Cycle Threshold (dCT) values to determine statistical significance.

For qPCR analysis, graphs plot mean ± CI. Statistical significance was determined using a two-tailed Student's *t*-test run on the dCT values. A P value <0.05 was considered statistically significant.

Results

Our previous studies have shown that CNTF has a potent effect in preventing the development of hypoxia-induced preretinal neovascularization.[27] It remains unclear whether this observed result represents a disease-specific effect of CNTF modulating the inner vascular plexus or if CNTF exerts a general antiangiogenic effect that also applies to the outer retina. To address this question, we tested recombinant rat CNTF in multiple angiogenesis models in the eye.

CNTF Prevents NV Development in the *Vldlr*$^{-/-}$ Model

In the *Vldlr*$^{-/-}$ model, a well-established model for retinal angiomatous proliferation, retinal neovascularization originates from the deep and intermediate vascular plexus and dives down to the choroid to form retinal-choroidal anastomoses most likely due to a metabolic defect.[35,36] When *Vldlr*$^{-/-}$ mice were treated with intravitreal injections of 500 ng CNTF at P12 before the onset of NV formation, the amount of NV at P18 is decreased by 60% in the CNTF-treated group compared to controls (Fig. 1A). However, treatment with lower concentrations of CNTF (5 ng) did not prevent intraretinal NV formation. Despite the short half-life of the recombinant protein, the treatment effect of CNTF injected at P12 was even more pronounced 22 days postinjection (P34), represented by a 75% decrease in NV in CNTF-treated eyes compared to controls (Fig. 1B). Delayed treatment with intravitreal CNTF at P19, a timepoint when NV are fully established, did not induce a decrease in intraretinal NV at P34.

CNTF Prevents CNV Development and Delays Formation of the Vascular Deep Plexus

In the laser-CNV model, retinal photocoagulation with an Argon laser induces choroidal neovascularization. Intravitreal injections of 500 ng CNTF 1 day postlaser significantly decreased CNV formation 7 days postlaser (Fig. 1C) while 5 ng CNTF again failed to provide a rescue effect. CNTF, therefore, strongly interferes with the development of pathologic neovascularization originating from the superficial[27] and deep retinal vascular plexus as well as the choroidal plexus in various retinal disease models. Given these data suggesting that CNTF has generalized antiangiogenic effects on vasculature throughout the retina, we hypothesized that CNTF also affects the retinal vascular development. To test this hypothesis, CNTF was injected intravitreally into wild-type mice at P7 and deep plexus formation was analyzed at P12. Figure 1D shows that injection of CNTF significantly delayed the formation of the deep vascular plexus at P12, confirming that CNTF affects angiogenesis during retinal development as well as in retinal disease.

CNTF Treatment Induces Long-Term Activation of the Jak/STAT3 Signaling Pathway in the *Vldlr*$^{-/-}$ Model

Considering the short half-life of CNTF when administered as recombinant protein,[27,37] the long-lasting effect of CNTF treatment on attenuating NV development in the *Vldlr*$^{-/-}$ model was unexpected. Since Jak/STAT3 signaling is strongly activated through CNTF, we hypothesized this signaling axis to play a role in mediating the long-lasting angiostatic effect of CNTF in vivo. In the *Vldlr*$^{-/-}$ model, intravitreal CNTF injections significantly increased levels of phosphorylated STAT3 (pSTAT3) in whole retinal lysates as soon as 6 hours after treatment in comparison to PBS/BSA-treated controls (Fig. 2A). Levels of STAT3 remained significantly elevated at 6 days after intravitreal injection of CNTF. The levels of pSTAT3 trended higher in CNTF-treated mice relative to controls at 6 days, but this comparison did not reach statistical significance as there was increased pSTAT3 expression in control-treated eyes. During retinal development, increased protein levels of pSTAT3 were detected at P32 but not P17 (Supplementary Fig. S1B), suggesting that there is no endogenous activation of the STAT3 signaling pathway before P18. On qPCR, expression levels of CNTF and STAT3 increased over time while the JAK inhibitor of STAT3, known as suppressor of cytokine signaling 3 (SOCS3), was downregulated (Supplementary Fig. S1A).

Next, we used a STAT3-target mRNA gene expression array to screen for important downstream genes regulated by CNTF treatments. Figure 2B shows all downstream genes that were upregulated more than twofold following CNTF treatment 24 hours and 6 days postinjection. Compared to the control-treated group, the most strongly upregulated genes in total retinal lysates 24 hours after CNTF injection included C-X-C motif chemokine ligand 10 (CxCl10), SOCS3, and CCAAT enhancer binding protein delta (Cebpd), a bZIP transcription factor involved in inflammatory responses.[38] CxCl10 remained one of the most strongly upregulated STAT3-target genes 6 days after CNTF treatment. qPCR analysis confirmed that CxCl10 and SOCS3 were both significantly upregulated over time while VEGF levels remained unaffected (Fig. 2C).

Müller Cells Respond to CNTF Treatment

To identify CNTF-responsive cells in CNTF-treated *Vldlr*$^{-/-}$ mice, we used pSTAT3 as an immunohistochemical marker in retinal cryosections. Figure 3A shows that pSTAT3 staining was detected in the superficial vascular plexus, as previously reported,[27] as well as the inner nuclear layer (INL), where Müller cells are located.[39] Next, we tested the effect of CNTF on Müller cells in vitro using primary murine Müller cell cultures. On immunohistochemistry, primary murine Müller cells were identified by positive glutamine synthetase, inward rectifying potassium channel 4.1 (Kir4.1), and *cis*-retinaldehyde binding protein (CRALBP) staining (Supplementary Fig. S2A). These cells expressed gp130, LifRβ, and CNTF-Rα at the mRNA level in vitro (Supplementary Fig. S2B). CNTF treatment strongly activated pSTAT3 signaling in primary Müller cell cultures (Fig. 3B). Similar to their expression levels in vivo, CxCl10 and SOCS3 were strongly upregulated in CNTF-treated Müller cells on qPCR, whereas VEGF164 levels were mildly altered (Fig. 3C). To further investigate the CNTF-induced changes in the Müller cell secretome, conditioned media from CNTF- and control-treated primary Müller cells were screened using the Mouse Angiogenesis Proteome Profiler (for a complete list of analytes contained on this array, please refer to Supplementary Table S1). As shown by the representative Proteome arrays in Figure 3D, the protein level of CxCl10 was higher in media conditioned by CNTF-treated Müller cells than control-treated cells. Quantitative analysis using ELISA confirmed that CxCl10 was significantly increased in CNTF-treated Müller cell-conditioned media. Taken together,

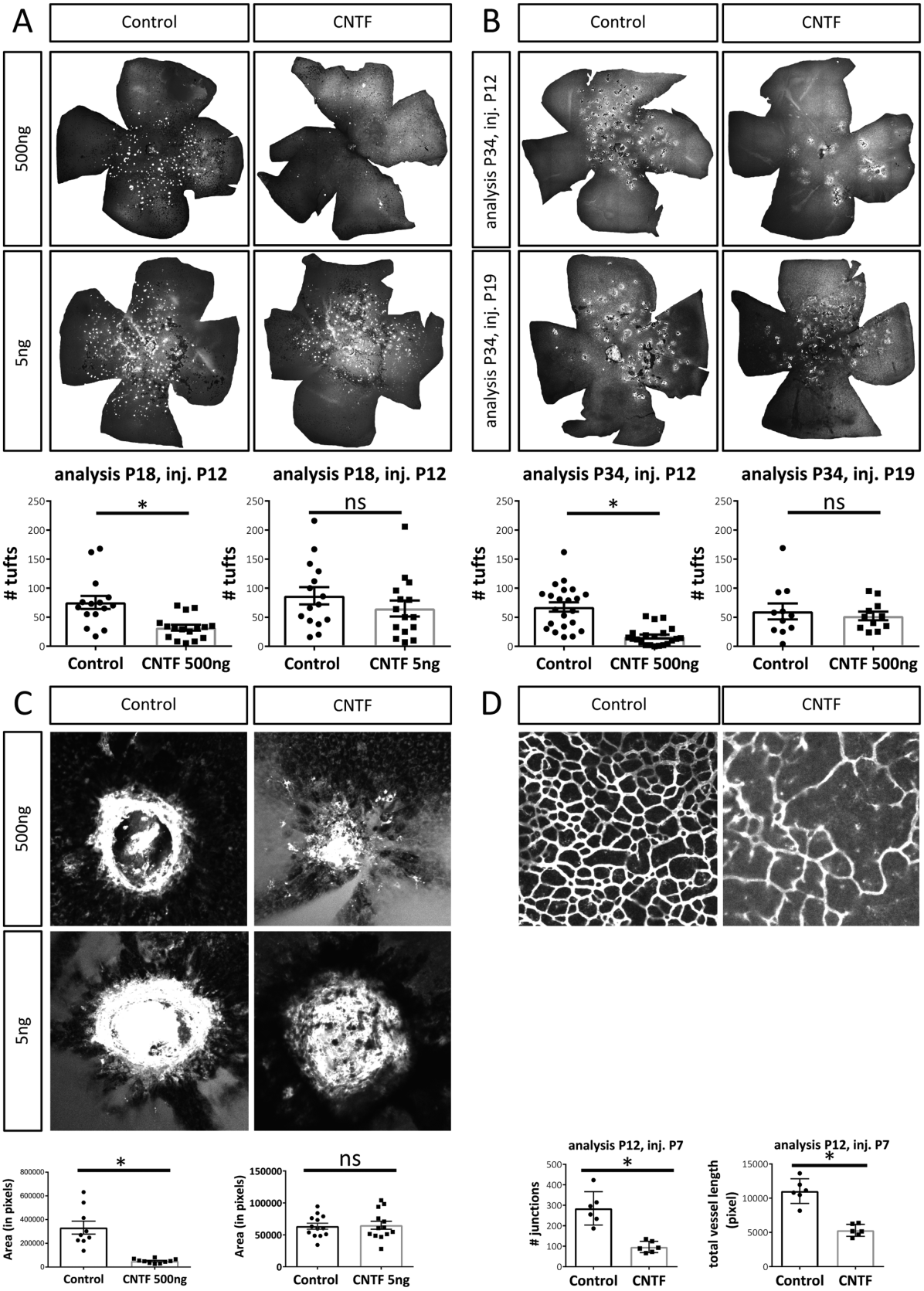

Figure 1. CNTF affects angiogenesis in the eye. (**A**) Representative flatmounts and quantification of NV tufts in *Vldlr*$^{-/-}$ mice at P18 following intravitreal treatment with 500 ng CNTF or 5 ng CNTF at P12. *n* (500 ng) = 16 mice, *n* (5 ng) = 15 mice, two-sided Student's *t*-test: **P* < 0.05. (**B**) Representative flatmounts and quantification of intraretinal NV in *Vldlr*$^{-/-}$ mice at P34 following intravitreal injections of 500 ng CNTF at P12 or P19. *n* (P34 inj P12) = 21 mice, *n* (P34 inj P19) = 11 mice, two-sided Student's *t*-test: **P* < 0.05. (**C**) Representative images and

quantified area of CNV lesions 7 days after laser injury following intravitreal injections of 500 ng or 5 ng CNTF 1 day after laser treatment. n (500 ng) = 10 retinas, n (5 ng) = 13 retinas, two-sided Student's t-test: $^*P < 0.05$. (**D**) Representative flatmounts and quantification of deep vascular plexus formation by the number of junctions at P12 following CNTF treatment (500 ng) at P7. $n = 6$ mice, two-sided Student's t-test: $^*P < 0.05$.

these data suggest that Müller cells increase secretion of CxCl10 in response to CNTF treatment.

CxCl10 Has an Angiostatic Effect in Vasoproliferative Disease Models of the Eye

CxCl10 is an interferon-inducible chemokine best known for its chemoattractant effect on T cells and leukocytes. CxCl10 has previously been shown to have angiostatic properties as well.[40,41] Based on our results showing that CNTF increases CxCl10 expression in retinal Müller cells, we hypothesized that Müller cell–secreted CxCl10 may be an important factor mediating the CNTF-induced angiostatic effect in retinal vasoproliferative disease models. In vitro, we confirmed that CxCl10 significantly inhibits endothelial cell proliferation and endothelial cell sprouting (Figs. 4A, 4B). This angiostatic effect was not limited to VEGF-induced sprouting but was also observed in bFGF-induced sprouting. In vivo, intravitreal injections of CxCl10 into *Vldlr*$^{-/-}$ mice at P12 led to a significant decrease in intraretinal NV at P18 (Fig. 4C). The angiostatic effect of CxCl10 was confirmed in the laser-CNV model where CxCl10-injected eyes demonstrated significantly smaller CNV lesions in comparison to control-treated eyes (Fig. 4D). These data show that CxCl10 has an angiostatic effect in the retina and support our hypothesis that CxCl10 is one of the factors mediating the CNTF-induced angiostatic effect in vasoproliferative retinal diseases.

Discussion

CNTF showed a significant treatment effect in multiple disease models of retinal angiogenesis (OIR, *Vldlr*$^{-/-}$ mice, laser-CNV) originating from different vascular layers and driven by distinct mechanisms. This observation suggests that the antiangiogenic properties of CNTF are attributable to a general effect rather than a disease-specific effect. To our knowledge, no other reports on CNTF's antiangiogenic properties outside the eye have been published, although Pasquin et al.[42] have recently shown that cardiotrophin-like cytokine factor 1, another CNTF-Rα ligand signaling through STAT3, also exerts a strong angiomodulatory effect in the OIR model. In comparison to our previously published observation that 5 ng CNTF significantly reduced preretinal NV in the OIR model, in our current study, higher CNTF concentrations were necessary to induce significant treatment effects in angiogenesis models of the outer retina and choroid.[27] This may be explained by the short half-life of the recombinant protein, which may lead to significantly lower CNTF concentrations in the outer retina compared to the vitreoretinal interface. Extensive dose-response experiments and determination of CNTF levels in the outer retina and choroid following intravitreal CNTF injections would be necessary to further address this hypothesis, although the variability of in vivo models may make the characterization of dose-response effects cumbersome.

In the *Vldlr*$^{-/-}$ model, CNTF showed a long-term treatment effect (Fig. 1B) that may be explained by its sustained activation of the Jak/STAT3 signaling pathway (Figs. 2A, 2B). The therapeutic success seems, however, to be time sensitive since significant reduction of NV was observed when CNTF was injected at P12 but not at P19 (Fig. 1B). Considering the fact that intraretinal NV in the *Vldlr*$^{-/-}$ model starts to develop around P14, CNTF prevented the development of NV but was not able to induce regression of preexisting NV. While retinal neovascular abnormalities spontaneously regress in the OIR and CNV model, the *Vldlr*$^{-/-}$ model is characterized by neovascular changes that persist over the long term.[35,43] Since the long-term effect of CNTF on the vascular phenotype was observed solely in the *Vldlr*$^{-/-}$ model in this study, our data cannot definitively conclude whether these prolonged effects are transferrable to other disease models of angiogenesis or are specific to the *Vldlr*$^{-/-}$ vasculopathy.

The short half-life of CNTF as recombinant protein has been well characterized,[37] whereas the long-lasting activation of that STAT3-signaling pathway in vivo is a novel observation. Rhee et al.[44] described a rapid decline in pSTAT3 levels in CNTF-treated dissociated P0 retinal cells after 90 minutes of treatment. The difference between these data and our results may lie in the difference between their ex vivo experimental setup on retinal tissue versus our in vivo design or the differences in time point of treatment (P0 versus P12), which greatly affects the status of retinal maturation.

In our previous work, we identified SOCS3 as a CNTF-induced endogenous inhibitor of cell proliferation in vascular endothelial cells.[27] Multiple studies have shown that Müller cells also respond to CNTF treatment with activation of the STAT3 signaling pathway, which corroborates our current findings in vivo as well as in vitro (Figs. 3A, 3B).[25,26,45] Immunohistochemical staining of pSTAT3 in retinal cryosections following CNTF treatment suggests that multiple retinal cell types, including Müller cells, respond to CNTF (Fig. 3A). While only a few bright nuclear pSTAT3 signals can be identified in the INL and ganglion cell layer (GCL), direct comparison of the control and CNTF-treated sample indicates a general shift in the pSTAT3 staining pattern from a nonspecific cytoplasmic labelling pattern in the control-treated sample to a more pronounced nuclear staining pattern in a variety of cell types within the INL and GCL in the CNTF-treated sample. We believe that this widespread pronounced nuclear label represents a positive response of multiple cell types to CNTF treatment. The difference between the clear increase in pSTAT3 signal in CNTF-treated samples in Western blot analysis and the moderate increase in nuclear pSTAT3 labeling in multiple cell types by immunohistochemistry may be explained by the technical challenges that come with immunohistochemical detection of phosphorylated proteins. These challenges include a different detection threshold when using immunohistochemistry as compared to Western blot analysis. In CNTF-treated samples, less pronounced nuclear pSTAT3 labels could be found throughout different layers of the INL, suggesting that multiple cell types in the INL respond to CNTF. Since the immunohistochemical images we have provided only allow for indirect identification of CNTF-responsive cells based on the nuclear localization in

Investigative Ophthalmology & Visual Science

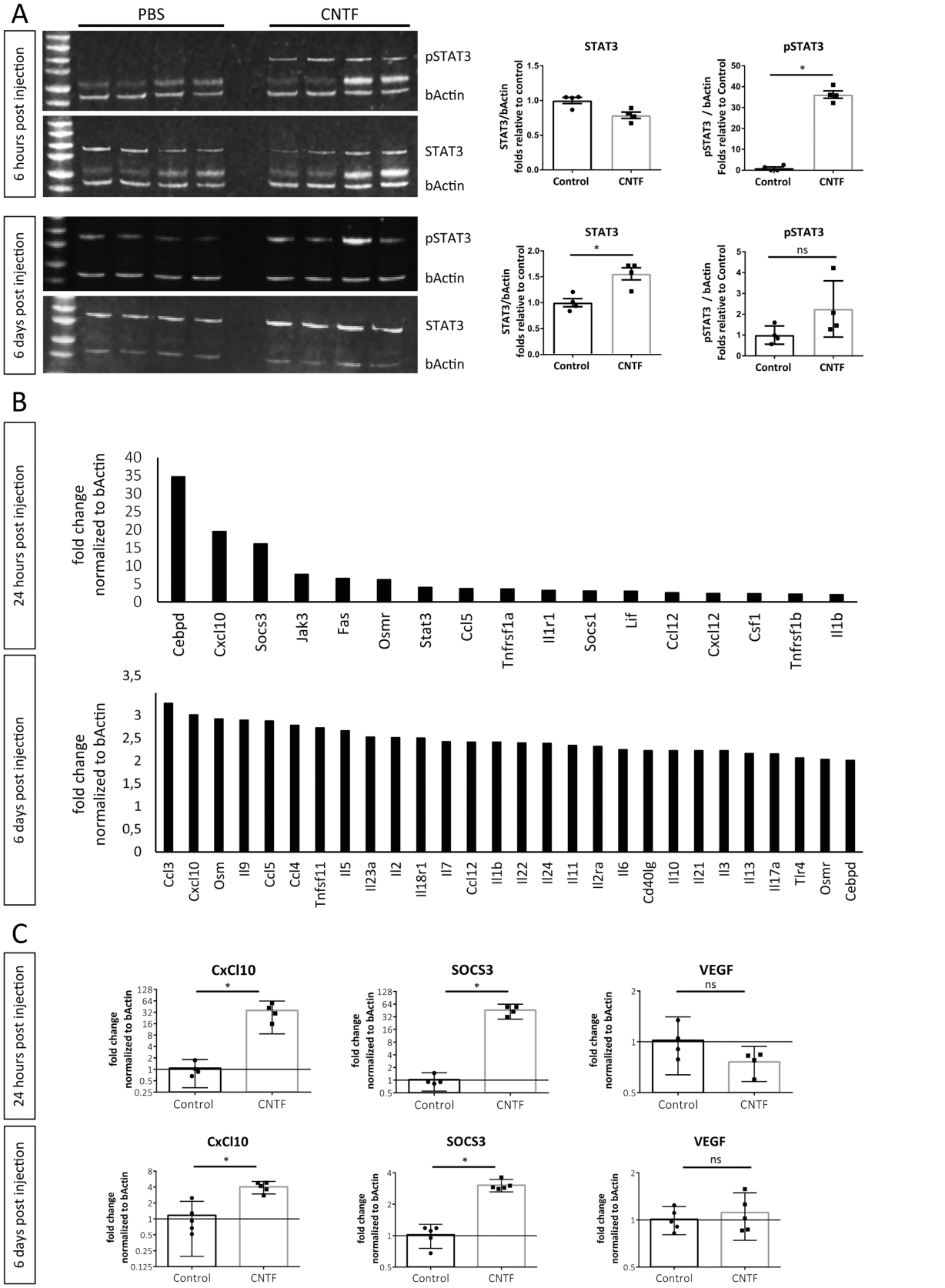

Figure 2. CNTF induces long-term activation of the Jak/STAT3 signaling pathway in *Vldlr*$^{-/-}$ mice. (**A**) pSTAT3, STAT3, and β-actin levels of retinal lysate 6 hours or 6 days after intravitreal injections with 500 ng CNTF or PBS/BSA vehicle control. Each column represents one biological replicate. $n = 4$ mice per group and time point. *$P < 0.05$, two-tailed Mann-Whitney test. (**B**) STAT3 targets upregulated more than twofold following 24 hours and 6 days after CNTF treatment identified using a STAT3 mRNA array on whole retinal lysates. $n = 3$ mice per group and per time point. (**C**) qPCR analysis of selected targets genes comparing expression levels between CNTF and control-treated eyes. $n = 4$–5 mice per group and per time point. Two-sided Student's t-test: *$P < 0.05$. All experiments were performed in the *Vldlr*$^{-/-}$ model.

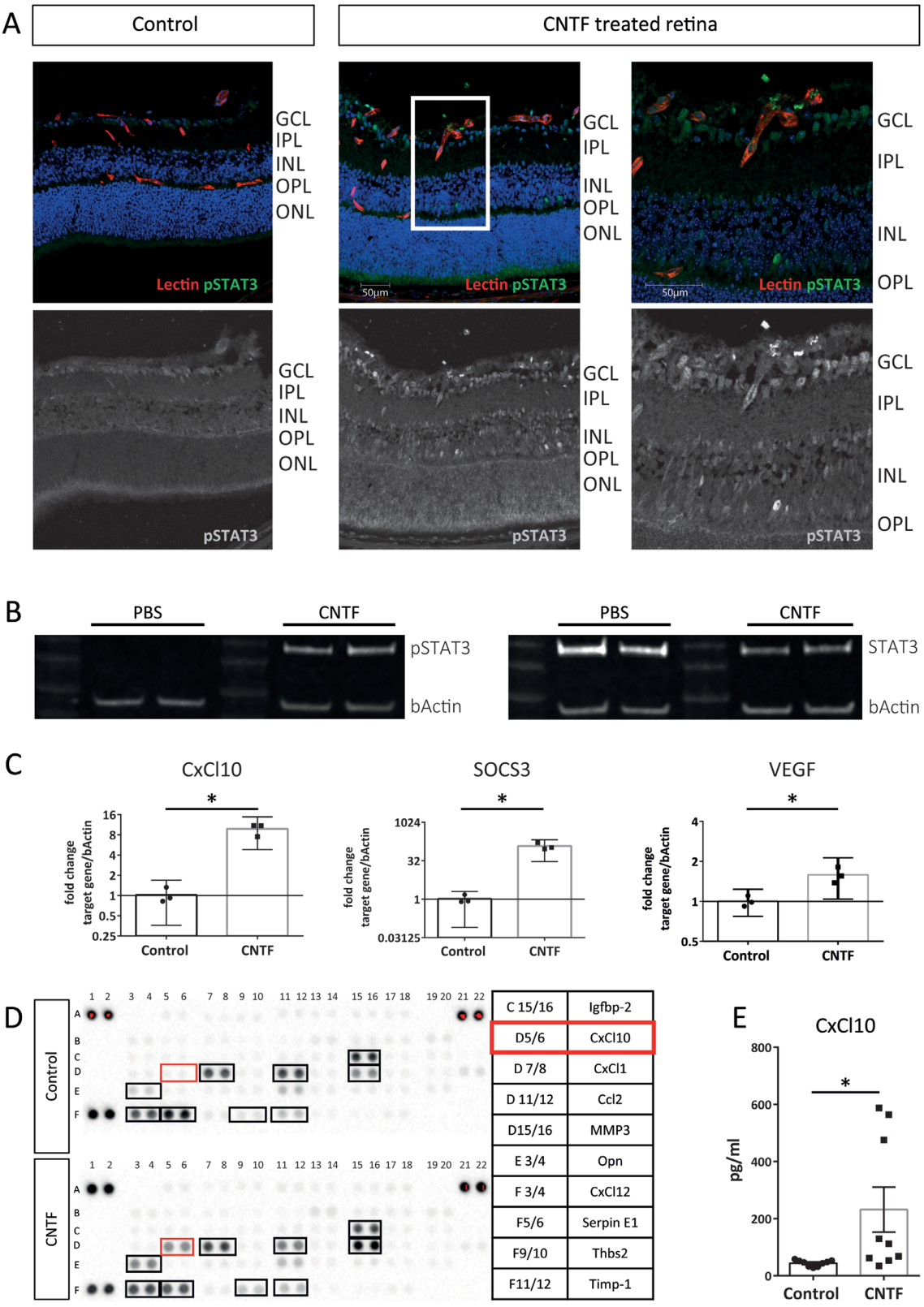

Figure 3. CNTF activates the JAK/STAT3 signaling pathway in Müller cells. (**A**) Immunohistochemical staining for pSTAT3 as a marker for STAT3 activation in retinal cryosections following CNTF treatment compared to untreated controls. (**B**) Western blot analysis for pSTAT3 levels in primary Müller cells 10 minutes after exposure to CNTF compared to untreated controls. (**C**) qPCR analysis shows gene expression of selected STAT3 target genes in primary Müller cells 1 hour post-CNTF treatment. Graphs show representative results of three independent experiments. Two-sided Student's *t*-test: $^*P < 0.05$. (**D**) Proteome profiler Mouse Angiogenesis Array comparing Müller cell–conditioned media of CNTF-treated Müller cells versus PBS control-treated cells. Opn, osteopontin; Thbs2, thrombospondin; $n = 1$ assay. (**E**) ELISA assay quantifying CxCl10 levels in Müller cell–conditioned media with and without CNTF treatment. $n = 9$ samples, two-sided Student's *t*-test: $^*P < 0.05$.

Investigative Ophthalmology & Visual Science

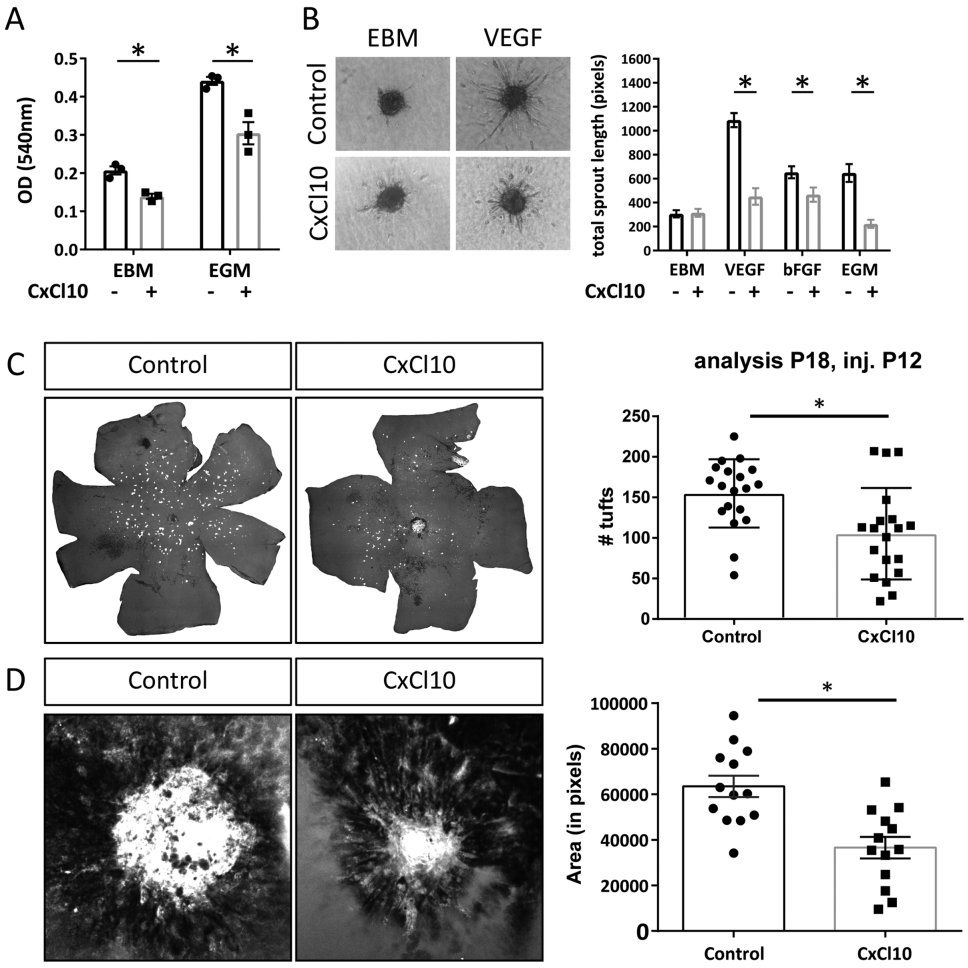

Figure 4. CxCl10 inhibits endothelial cell proliferation in vitro and in vivo. (**A**) MTT assay results of HUVECs after exposure to CxCl10 (537.5 ng/mL) under basal (EBM) and growth (EGM) stimulating conditions. $n = 3$ independent experiments, two-way ANOVA, $^*P < 0.05$. (**B**) Endothelial cell sprouting of HUVECs in response to CxCl10 (537.5 ng/mL) under diverse proangiogenic stimuli ($n = 14$–28 spheroids per group, two-way ANOVA, $^*P < 0.05$). (**D**) NV at P18 following intravitreal injection of CxCl10 (500 ng) in *Vldlr*$^{-/-}$ at P12. $n = 19$ mice, two-sided Student's *t*-test: $^*P < 0.05$. (**E**) CNV area 7 days postlaser following intravitreal injection of CxCl10 (500 ng) 1 day after laser treatment. $n = 13$ eyes, two-sided Student's *t*-test: $^*P < 0.05$.

the INL that correspond to the nuclear localization of Müller cells and horizontal cells, in vitro experiments were necessary to elucidate the role of Müller cells in CNTF's angiomodulatory effect in the retina (Figs. 3B–3E, Supplementary Fig. S2). In this study, we chose to focus on the interaction of Müller glia and endothelial cells in the context of CNTF treatment; further studies will be necessary to investigate the role of neuronal cells of the INL and GCL (including ganglion cells) that are likely to contribute to the overall angiomodulatory effect of CNTF on the retina based on the observed widespread pSTAT3 signal in retina cryosections.

To characterize the molecular mechanism by which Müller cells activated by CNTF act on vascular endothelial cells, we ran an mRNA array on CNTF-treated whole retina lysates and compared the results with the results of a semiquantitative proteome profiler array of Müller cell–conditioned media following CNTF treatment. CxCl10 was strongly upregulated in both assays. These data were consistent with a study by Xue et al.,[46] who identified CxCl10 as one of multiple genes upregulated in sorted Müller cells following intravitreal treatment with CNTF. Interestingly, results on VEGF levels following CNTF treatment were inconsistent between in vivo and in vitro settings showing unaltered VEGF levels in vivo (Fig. 2C) and a 1.5-fold increase in VEGF levels in vitro (Fig. 3C). Our in vivo data are consistent with findings from previous study results in the OIR model showing no increase in retinal VEGF following CNTF treatment.[27] The modest VEGF increase in Müller cells in response to CNTF treatment may not be detectable in vivo since VEGF levels are determined in whole retinal lysates, where Müller cells represent only a small fraction of the total cell population. Taken together, these data support that CxCl10 may be an important mediator of CNTF's indirect Müller cell–mediated angiostatic effect on vascular endothelial cells.

While our mRNA array yielded results consistent with STAT3 activation following CNTF treatment, this study was limited to identifying established STAT3 targets like CxCl10. Other techniques such as RNA-Seq analysis or liquid chromatography/mass spectrometry on Müller cell–conditioned media will be necessary to identify further CNTF-induced STAT3 targets.

CxCl10's angiostatic effect has been well established, but its role in the retina remains unclear.[40,47] Increased levels of CxCl10 were found in the aqueous humor of patients with age-related macular degeneration.[48] Nawaz et al.,[49] however, found an association between levels of CxCl10 and resolution of angiogenesis with induction of fibrosis in patients with diabetic retinopathy. Ha et al.[50] suggested a role of CxCl10 in retinal inflammation and oxidative stress in response to retinal ischemia. Gao et al.[51] postulated an angiostatic effect of CxCl10 in inflamed corneas. Our data show that CxCl10 is capable of inhibiting retinal as well as choroidal neovascularization (Figs. 4C, 4D). These data align with results from Fujimura et al.,[52] who showed that loss of the CxCl10 receptor CxCR3 leads to an increase in NV area in the laser-CNV model. Interestingly, the observed CxCl10 treatment effect in the *Vldlr*$^{-/-}$ model as well as the laser-CNV model was smaller than the CNTF-induced treatment effects (Fig. 1A). In the *Vldlr*$^{-/-}$ model, the number of tufts was reduced to 42% (normalized to the mean of the control group) in CNTF-treated eyes compared to 68% in CxCl10-treated eyes. Normalized to the mean CNV area of the control-treated group of the laser-CNV model, the mean CNV area was reduced 85% in the CNTF-treated group and reduced 32% in the CxCl10-treated group. This clearly supports the hypothesis that Müller cell–secreted CxCl10 is one of the multiple factors besides endothelial SOCS3 that mediate CNTF's angiostatic effect in retinal vasoproliferative disease.

Acknowledgments

The authors thank Marc Guder (Eye Centre, University of Freiburg) as well as Mauricio Rosenfeld (The Scripps Research Institute) for excellent technical support.

Supported by grants to MF from the National Eye Institute (R01 EY11254 and R24 EY022025) and the Lowy Medical Research Institute (MacTel). FB was supported by the German Research Foundation (Bu3135/1-1) and the Dr. Werner-Jackstädt-Nachwuchspreis of the German Retina Society. KVM was supported by the National Eye Institute (F30 EY029131-01) and the University of California, San Diego Medical Scientist Training Program (T32 GM007198-40).

Disclosure: **F. Bucher**, None; **E. Aguilar**, None; **K.V. Marra**, None; **J. Rapp**, None; **J. Arnold**, None; **S. Diaz-Aguilar**, None; **C. Lange**, None; **H. Agostini**, None; **G. Schlunck**, None; **A. Stahl**, None; **M. Friedlander**, None

References

1. Bourne RR, Stevens GA, White RA, et al. Causes of vision loss worldwide, 1990–2010: a systematic analysis. *Lancet Global Health*. 2013;1:e339–e349.
2. Cheung N, Wong IY, Wong TY. Ocular anti-VEGF therapy for diabetic retinopathy: overview of clinical efficacy and evolving applications. *Diabetes Care*. 2014;37:900–905.
3. Krebs I, Glittenberg C, Ansari-Shahrezaei S, Hagen S, Steiner I, Binder S. Non-responders to treatment with antagonists of vascular endothelial growth factor in age-related macular degeneration. *Br J Ophthalmol*. 2013;97:1443–1446.
4. Suzuki M, Nagai N, Izumi-Nagai K, et al. Predictive factors for non-response to intravitreal ranibizumab treatment in age-related macular degeneration. *Br J Ophthalmol*. 2014;98:1186–1191.
5. Chatziralli IP, Sharma PK, Sivaprasad S. Treatment modalities for idiopathic macular telangiectasia: an evidence-based systematic review of the literature. *Semin Ophthalmol*. 2017;32:384–394.
6. Gantner ML, Eade K, Wallace M, et al. Serine and lipid metabolism in macular disease and peripheral neuropathy. *N Engl J Med*. 2019;381:1422–1433.
7. Ambati J, Atkinson JP, Gelfand BD. Immunology of age-related macular degeneration. *Nat Rev Immunol*. 2013;13:438–451.
8. Tang J, Kern TS. Inflammation in diabetic retinopathy. *Prog Retinal Eye Res*. 2011;30:343–358.
9. Gardner TW, Davila JR. The neurovascular unit and the pathophysiologic basis of diabetic retinopathy. *Graefe Arch Clin Exp Ophthalmol*. 2017;255:1–6.
10. Pardue MT, Allen RS. Neuroprotective strategies for retinal disease. *Prog Retinal Eye Res*. 2018;65:50–76.
11. Rubsam A, Parikh S, Fort PE. Role of inflammation in diabetic retinopathy. *Int J Mol Sci*. 2018;19:942.
12. Wen R, Tao W, Li Y, Sieving PA. CNTF and retina. *Prog Retinal Eye Res*. 2012;31:136–151.
13. Stahl N, Yancopoulos GD. The tripartite CNTF receptor complex: activation and signaling involves components shared with other cytokines. *J Neurobiol*. 1994;25:1454–1466.
14. Stahl N, Boulton TG, Farruggella T, et al. Association and activation of Jak-Tyk kinases by CNTF-LIF-OSM-IL-6 beta receptor components. *Science*. 1994;263:92–95.
15. Elson GC, Lelievre E, Guillet C, et al. CLF associates with CLC to form a functional heteromeric ligand for the CNTF receptor complex. *Nat Neurosci*. 2000;3:867–872.
16. Ip NY, McClain J, Barrezueta NX, et al. The alpha component of the CNTF receptor is required for signaling and defines potential CNTF targets in the adult and during development. *Neuron*. 1993;10:89–102.
17. Davis S, Aldrich TH, Valenzuela DM, et al. The receptor for ciliary neurotrophic factor. *Science*. 1991;253:59–63.
18. LaVail MM, Unoki K, Yasumura D, Matthes MT, Yancopoulos GD, Steinberg RH. Multiple growth factors, cytokines, and neurotrophins rescue photoreceptors from the damaging effects of constant light. *Proc Natl Acad Sci USA*. 1992;89:11249–11253.
19. Pease ME, Zack DJ, Berlinicke C, et al. Effect of CNTF on retinal ganglion cell survival in experimental glaucoma. *Invest Ophthalmol Vis Sci*. 2009;50:2194–2200.
20. Lipinski DM, Barnard AR, Singh MS, et al. CNTF gene therapy confers lifelong neuroprotection in a mouse model of human retinitis pigmentosa. *Mol Therapy*. 2015;23:1308–1319.
21. Li Y, Tao W, Luo L, et al. CNTF induces regeneration of cone outer segments in a rat model of retinal degeneration. *PLoS One*. 2010;5:e9495.
22. Tao W, Wen R, Goddard MB, et al. Encapsulated cell-based delivery of CNTF reduces photoreceptor degeneration in animal models of retinitis pigmentosa. *Invest Ophthalmol Vis Sci*. 2002;43:3292–3298.
23. Birch DG, Weleber RG, Duncan JL, Jaffe GJ, Tao W. Randomized trial of ciliary neurotrophic factor delivered by encapsulated cell intraocular implants for retinitis pigmentosa. *Am J Ophthalmol*. 2013;156:283–292.e281.
24. Chew EY, Clemons TE, Jaffe GJ, et al. Effect of ciliary neurotrophic factor on retinal neurodegeneration in patients with macular telangiectasia type 2: a randomized clinical trial. *Ophthalmology*. 2019;126:540–549.
25. Wen R, Song Y, Kjellstrom S, et al. Regulation of rod phototransduction machinery by ciliary neurotrophic factor. *J Neurosci*. 2006;26:13523–13530.

26. Rhee KD, Nusinowitz S, Chao K, Yu F, Bok D, Yang XJ. CNTF-mediated protection of photoreceptors requires initial activation of the cytokine receptor gp130 in Muller glial cells. *Proc Natl Acad Sci USA*. 2013;110:E4520–E4529.
27. Bucher F, Walz JM, Buhler A, et al. CNTF attenuates vasoproliferative changes through upregulation of SOCS3 in a mouse-model of oxygen-induced retinopathy. *Invest Ophthalmol Vis Sci*. 2016;57:4017–4026.
28. Lambert V, Lecomte J, Hansen S, et al. Laser-induced choroidal neovascularization model to study age-related macular degeneration in mice. *Nat Protocols*. 2013;8:2197–2211.
29. Zudaire E, Gambardella L, Kurcz C, Vermeren S. A computational tool for quantitative analysis of vascular networks. *PLoS One*. 2011;6:e27385.
30. Ueki Y, Karl MO, Sudar S, et al. P53 is required for the developmental restriction in Muller glial proliferation in mouse retina. *Glia*. 2012;60:1579–1589.
31. Mosmann T. Rapid colorimetric assay for cellular growth and survival: application to proliferation and cytotoxicity assays. *J Immunol Methods*. 1983;65:55–63.
32. Korff T, Augustin HG. Tensional forces in fibrillar extracellular matrices control directional capillary sprouting. *J Cell Sci*. 1999;112(pt 19):3249–3258.
33. Buehler A, Sitaras N, Favret S, et al. Semaphorin 3F forms an anti-angiogenic barrier in outer retina. *FEBS Lett*. 2013;587:1650–1655.
34. Banin E, Dorrell MI, Aguilar E, et al. T2-TrpRS inhibits preretinal neovascularization and enhances physiological vascular regrowth in OIR as assessed by a new method of quantification. *Invest Ophthalmol Vis Sci*. 2006;47:2125–2134.
35. Dorrell MI, Aguilar E, Jacobson R, et al. Antioxidant or neurotrophic factor treatment preserves function in a mouse model of neovascularization-associated oxidative stress. *J Clin Invest*. 2009;119:611–623.
36. Joyal JS, Sun Y, Gantner ML, et al. Retinal lipid and glucose metabolism dictates angiogenesis through the lipid sensor Ffar1. *Nat Med*. 2016;22:439–445.
37. Dittrich F, Thoenen H, Sendtner M. Ciliary neurotrophic factor: pharmacokinetics and acute-phase response in rat. *Ann Neurol*. 1994;35:151–163.
38. Balamurugan K, Sterneck E. The many faces of C/EBPdelta and their relevance for inflammation and cancer. *Int J Biol Sci*. 2013;9:917–933.
39. Bringmann A, Pannicke T, Grosche J, et al. Muller cells in the healthy and diseased retina. *Prog Retinal Eye Res*. 2006;25:397–424.
40. Luster AD, Greenberg SM, Leder P. The IP-10 chemokine binds to a specific cell surface heparan sulfate site shared with platelet factor 4 and inhibits endothelial cell proliferation. *J Exp Med*. 1995;182:219–231.
41. Angiolillo AL, Sgadari C, Taub DD, et al. Human interferon-inducible protein 10 is a potent inhibitor of angiogenesis in vivo. *J Exp Med*. 1995;182:155–162.
42. Pasquin S, Chehboun S, Dejda A, et al. Effect of human very low-density lipoproteins on cardiotrophin-like cytokine factor 1 (CLCF1) activity. *Sci Rep*. 2018;8:3990.
43. Hu W, Jiang A, Liang J, et al. Expression of VLDLR in the retina and evolution of subretinal neovascularization in the knockout mouse model's retinal angiomatous proliferation. *Invest Ophthalmol Vis Sci*. 2008;49:407–415.
44. Rhee KD, Goureau O, Chen S, Yang X-J. Cytokine-induced activation of signal transducer and activator of transcription in photoreceptor precursors regulates rod differentiation in the developing mouse retina. *J Neurosci*. 2004;24:9779–9788.
45. Peterson WM, Wang Q, Tzekova R, Wiegand SJ. Ciliary neurotrophic factor and stress stimuli activate the Jak-STAT pathway in retinal neurons and glia. *J Neurosci*. 2000;20:4081–4090.
46. Xue W, Cojocaru RI, Dudley VJ, Brooks M, Swaroop A, Sarthy VP. Ciliary neurotrophic factor induces genes associated with inflammation and gliosis in the retina: a gene profiling study of flow-sorted, Muller cells. *PLoS One*. 2011;6:e20326.
47. Campanella GSV, Colvin RA, Luster AD. CXCL10 can inhibit endothelial cell proliferation independently of CXCR3. *PLoS One*. 2010;5:e12700.
48. Liu F, Ding X, Yang Y, et al. Aqueous humor cytokine profiling in patients with wet AMD. *Mol Vis*. 2016;22:352–361.
49. Nawaz MI, Van Raemdonck K, Mohammad G, et al. Autocrine CCL2, CXCL4, CXCL9 and CXCL10 signal in retinal endothelial cells and are enhanced in diabetic retinopathy. *Exp Eye Res*. 2013;109:67–76.
50. Ha Y, Liu H, Xu Z, et al. Endoplasmic reticulum stress-regulated CXCL10/CXCR3 pathway mediates inflammation and neuronal injury after retinal ischemia. *Invest Ophthalmol Vis Sci*. 2014;55:2178–2178.
51. Gao N, Liu X, Wu J, et al. CXCL10 suppression of hem- and lymph-angiogenesis in inflamed corneas through MMP13. *Angiogenesis*. 2017;20:505–518.
52. Fujimura S, Takahashi H, Yuda K, et al. Angiostatic effect of CXCR3 expressed on choroidal neovascularization. *Invest Ophthalmol Vis Sci*. 2012;53:1999–2006.

Investigative Ophthalmology & Visual Science